Electric solar wind sail

ESAIL D23.3
Tether vacuum-testing results

Work Package: **WP 23**

Version: **Version 1.0**

Prepared by: Taneli Kalvas, Olli Tarvainen, Hannu Koivisto and Pekka Janhunen

Time: Jyväskylä, November 7th, 2013

Coordinating person: Hannu Koivisto, hannu.koivisto@phys.jyu.fi

(List of participants:)

Participant no.	Participant organisation	Abbrev.	Country
1	Finnish Meteorological Institute	FMI	Finland
3. (Coordinator)	University of Jyväskylä	UJ	Finland

Table of Contents

1. Introduction

The E-sail tether is subject to the harsh conditions of outer space, including high photon flux from the sun. In addition, during E-sail operation it is biased to +20 - 40 kV positive potential with respect to the surrounding solar wind plasma, which causes solar wind electrons to bombard its surface. The most important phenomena affecting the tether in space that need to be considered have been judged to be the temperature equilibrium of the tether, effects of the electron bombardment and spark resistivity.

The tether to be used in E-sail is developed by University of Helsinki. The tether will be a *Heytether* construction made out of one 50 μm main wire and several 25 μm auxiliary wires, which are periodically bonded to the main wire with ultrasonic bonding technique to increase the micrometeoroid tolerance of the tether structure. The baseline material choice for the tether is standard bonding wire aluminium, which is an alloy of 99 % Al and 1 % Si. The tether manufacturing and tether coating developments have been made in work packages 2.1 and 2.2. The tether wire coating tested in this work is 100 nm aluminium oxide Al_2O_3 grown by atomic layer deposition (ALD). The tether structure is not relevant for testing the materials and coating. Therefore for simplicity a single 25 μm and 50 μm aluminium wires have been used for testing.

2. Temperature equilibrium of tether

2.1. Test motivation

One of the most important things impacting the life-time or durability of the tether is it's equilibrium temperature. The temperature affects the material properties of the aluminum wire under tension, for example creep, tensile strength and other mechanical properties. The equilibrium temperature of the tether in space depends highly on the emissivity of the tether as radiation is the only heat loss mechanism for such long and thin structure. Data book values for emissivity are 0.03 for polished and clean aluminium [1] and >0.2 for typical bulk Al_2O_3 [2], but unfortunately the use of bulk data to such small structures as the tethers and the nanometer scale coating is somewhat dubious. According to Wien's displacement law the most intensive photon wavelength for the radiation from a body at 600 K is 4.8 μm, for example and the aluminium oxide thickness is at least an order of magnitude smaller than the wavelength. Therefore it is sure that the emissivity of the bulk aluminium oxide is not applicable. Because of this the emissivity of the tether wire has to be measured.

2.2. Emissivity measurement setup

An experimental setup has been designed and prepared for measuring the emissivity and making the electron bombardment in the same vacuum chamber. In this way the emissivity of the tether wire can be measured after bombardment without exposing the tether to air, which could cause oxidation or other changes in the aluminium wire or the coatings. The testing was done using a 30 cm high, 50 cm diameter vacuum chamber with many ports for the necessary voltage feed-throughs for tests (see figure 1). The emissivity measurements were made at a pressure of $<4\cdot10^{-6}$ mbar.

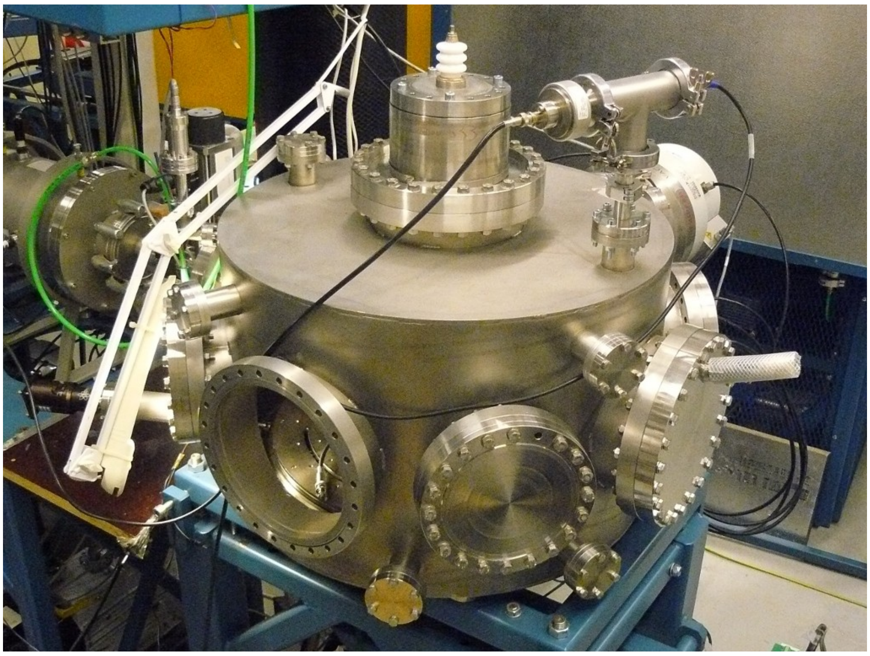

Figure 1. The vacuum chamber where tether testing was performed.

The basic idea for measuring the emissivity of the tether wire is to heat up the wire in vacuum conditions while measuring voltage drop across the wire for getting a resistance value, which is a function of the wire temperature. The emissivity value has a strong effect on the thermodynamics of the wire because the wire is long compared to its diameter and therefore the heat conduction is low compared to radiated heat. Because of the boundary effects, non-constant resistivity of aluminium, power-law dependence of radiation, etc. the only way to get the emissivity of the wire is to compare the experimental data to data from a computer simulation.

The measurements were done in a vacuum chamber shown in figure 2 with low 10^{-7} mbar pressure. The wire under measurement is bonded to 15x10x1 mm^3 aluminium plates (plate A) at each end, which are bolted to a larger aluminium plates (plate B) used to mechanically connect the measurement wire to a rigid support frame keeping the wire approximately straight (see figure 2). The plate B at each end is used to connect the measurement wires coming from the vacuum feed-throughs. Outside the vacuum the electronics shown in figure 3 is connected to the measurement wires. The electronics uses a four-wire connection. Two of the wires are used for the bias current and two of the wires are used to voltage measurement. Therefore the biggest other contribution to the measured resistance comes from contact resistance between plate A and the wire (the bonded contact). The measurement electronics is connected to computer control/DAQ system National Instruments PCI-6229, which is used to collect data at 10 kHz sample rate. Calibration of the device was done with 10 ohm and 100 ohm 1 % resistors and Fluke 87 IV multimeter by driving the measurement current through the resistor and measuring the voltage drop with the multimeter. Current setting and voltage reading calibration coefficients were set accordingly.

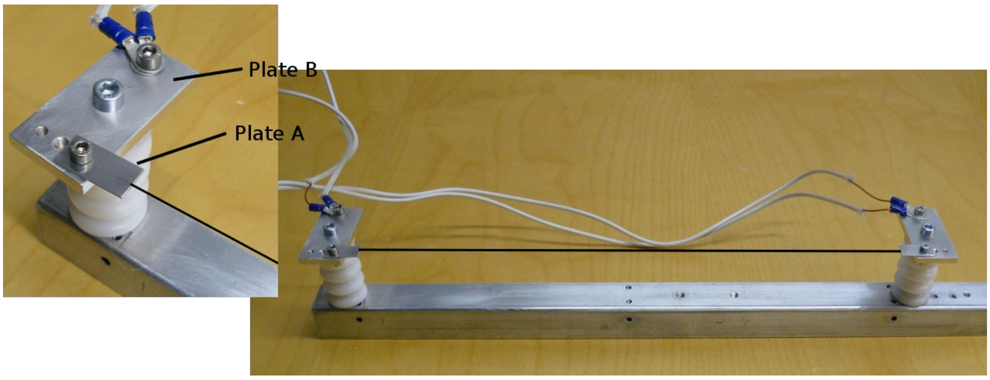

Figure 2. Emissivity measurement setup inside vacuum chamber. The tether wire under measurement is bonded to plate A, which is bolted to plate B, where the electrical connections are made. The tether wire thickness is exaggerated in the image.

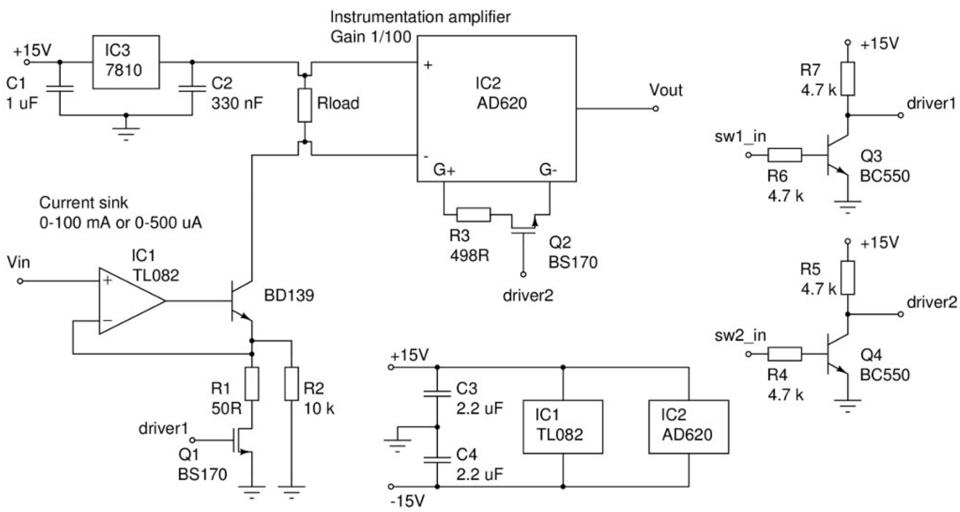

Figure 3. Circuit schematics of electronics developed for emissivity measurement. The electronics provides a four-wire resistance meter functionality with two ranges for currents and two gain settings.

2.3. Simulation program

The simulation program used for modelling the heated tether wire is based on solution of heat equation in a one-dimensional system, where resistive heating, heat conductance and radiative losses are taken in account. The simulation discretizes the wire of length L into N (nominal value 100) cylindrical pieces or nodes, which are assumed to have a temperatures T_i. Each cylinder therefore has a length Δx. The systems is iterated with Δt time steps from a starting point of fixed T=300 K. At each time step, the temperatures of the nodes are updated according to a local energy flow: $\Delta T = P\ \Delta t / (c(T_i)\cdot\rho\cdot A\cdot\Delta x)$, where $c(T)$ is the heat capacity of aluminum as a function of temperature, ρ is the density of aluminum, A is the cross section of the aluminum wire and P is the sum of heat fluxes to the node. The heat flux calculation is made taking in account the heat conductance $k(T)$ as a function of temperature and the emissivity is assumed to be a linear function of temperature $E(T)=E_A+E_B\cdot T$. The ends of the wire are assumed to be in fixed temperature 300 K (equals to 26 C, which is within +/-2 C of the laboratory temperature). The heat flux to the ends is observed and the corresponding temperature rise of the plate A is calculated assuming that no heat is conducted away from the system. These temperature rises have been under 0.5 K in all cases.

In the simulations, data for pure 100 % aluminium has been used even though the tether material is 1 % silicon. This additional approximation had to be made as the relevant data has not been found (as a function of temperature) for the alloy in question.

2.4. Measurements and analysis

All emissivity measurements have been made using the same measurement sequence, but with different current values. For 25 µm wire the heating currents were: 1 mA, 5 mA, 10 mA, 15 mA and 20 mA and the low current for resistance measurement was 50 µA. For 50 µm wire the heating currents were: 5 mA, 10 mA, 20 mA, 40 mA and 60 mA and the low current for resistance measurement was 320 µA. Each measurement consists of (a) 1 second of background measurement with zero bias, (b) 1 second of resistance measurement with low current, (c) 200 seconds of heating, (d) 200 seconds of resistance measurement with low current and (e) 600 seconds of cooling with zero current before next measurement cycle.

The data fitting was done by a computer program minimizing the χ^2 deviation of the simulation and the measurement with Nelder-Mead nonlinear simplex algorithm. The free parameters in the fit were the wire thickness and the two coefficients E_A and E_B for emissivity. Emissivity was assumed to be a linear function of temperature $E(T)=E_A+E_B\cdot T$. The fitting was done at the static situation when heating is on (time 100-200 s). The wire thicknesses achieved this way were between 24.7 and 25.2 µm for nominally 25 µm wires and between 48.9 µm and 52.0 µm for nominally 50 µm wires. The measured resistances for 21.12.2011 test are plotted in figure 4 together with fitted simulation results. In figure 5 the temperature profiles of the wire according to the simulations is presented.

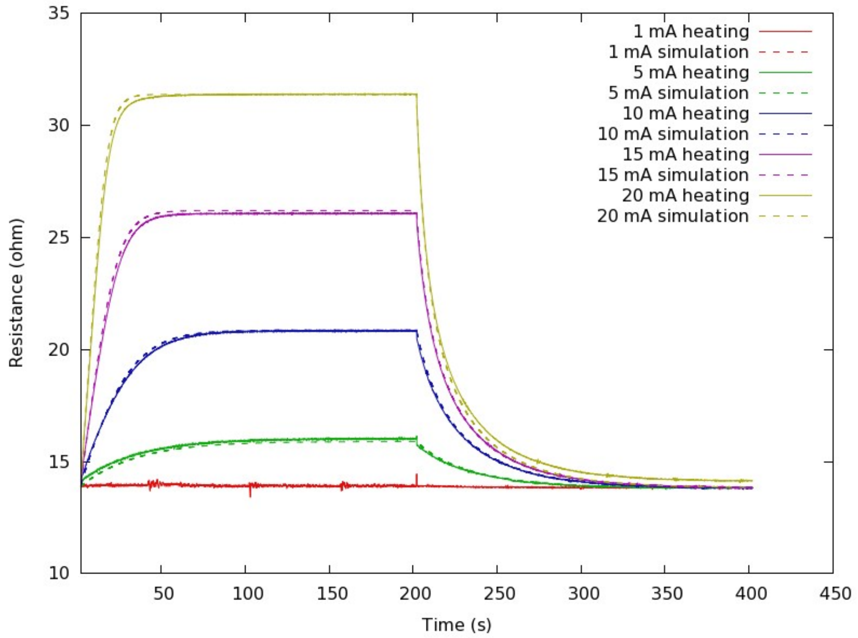

Figure 4. Resistance of the 246 mm long 25 µm diameter tether wire in the emissivity measurement sequence for five different heating currents.

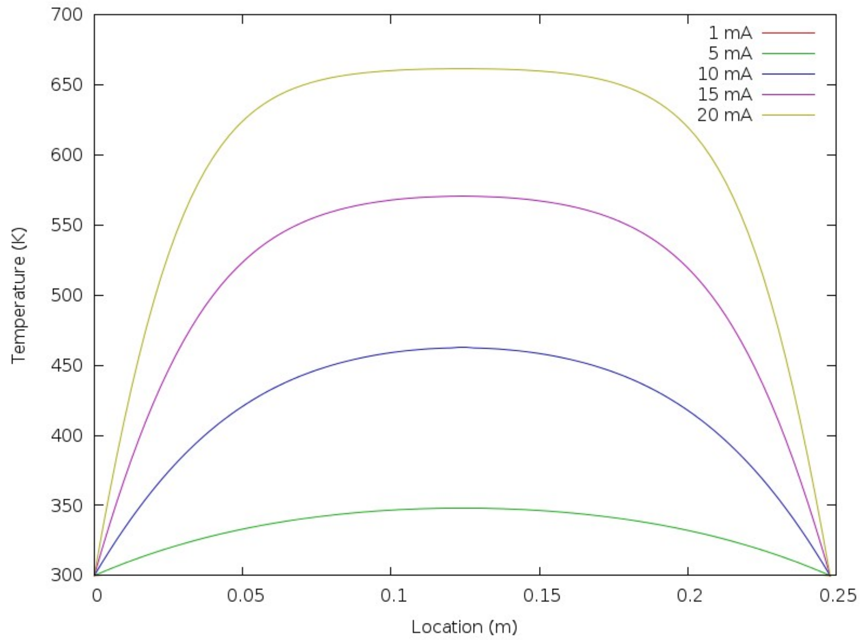

Figure 5. Temperature profile along the wire according to the simulations in the 21.12.2011 test.

All the measured emissivities as a function of temperature are plotted in figure 6 together with data from Engineering toolbox for unoxidized aluminium [1]. The temperature range, which has been used in measurements is between 300 and

650 K. The plot is extended to 1000 K to include the third Engineering toolbox data point. The emissivity coefficient are also presented in table 1.

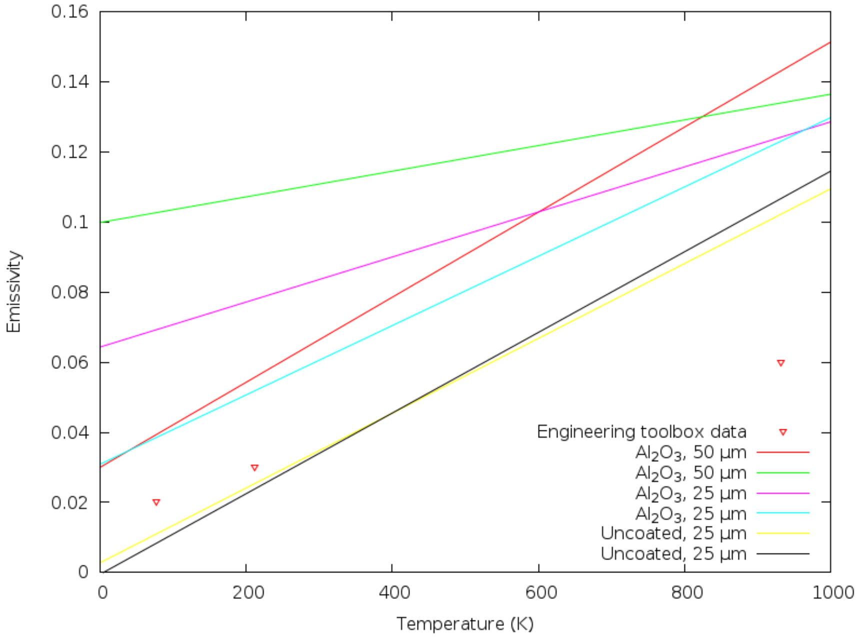

Figure 6. Measured emissivities of the tether wire samples together with three data points from literature.

Table 1. The fitted emissivity coefficients.

	E_A	E_B
Al_2O_3 50 µm (16.10.2013)	0.0300264	0.0001213
Al_2O_3 50 µm (28.10.2013)	0.0998565	0.0000365
Al_2O_3 25 µm (27.02.2012)	0.0643278	0.0000642
Al_2O_3 25 µm (17.02.2012)	0.0309143	0.0000988
Uncoated, 25 µm (21.12.2011)	0.00280739	0.0001066
Uncoated, 25 µm (07.12.2011)	-0.00354228	0.0001150

3. Tether electron bombardment

3.1. Theoretical analysis

According to the NIST ESTAR program [3], the stopping power for 20 keV electrons in aluminium is 2700 eV/µm and the range is 4.3 µm. In aluminium oxide the stopping power is 4100 eV/µm and range is 2.8 µm. Therefore the electrons are fully stopped close to the wire surface. In a head-on collision with Al or O, the energy transmitted to an atom is not sufficient to cause displacement damage.

Therefore the only effect that the electrons may have on the material is due to displacement of electrons. In aluminium this has no effect as it is a conductor, but in Al_2O_3 the electron displacement leads to formation of holes and breakage of Al-O bonds. If the Al_2O_3 layer is 100 nm thick, each incident electron will displace 80 bound electrons on average. This results for example in the high secondary electron emission observed in Al_2O_3 [4]. Overall, in the E-sail application, with 0.1 mA electron current to a 20 km 50 µm tether wire, each oxygen atom in the tether coating will experience about 90 events per year, where its bond electrons participate in collisions with incident electrons. This will lead to ejection of oxygen atoms from the surface as they become weakly bound, unless processes exist, which provide electrons to the hole sites faster than they are created. It may be that the strong UV light radiation in space excites electrons to the conduction band, which then seek the hole sites. The hole sites may also be filled by UV induced photoelectrons, which are drawn towards the wire due to the biasing. Unfortunately the rate of such processes is not known. If significant ejection of oxygen atoms from the surface happens, the relative amount of Al atoms in the surface will increase. This will bring the emissivity closer to emissivity of bulk aluminium.

3.2. Description of experiment

The durability of the Al_2O_3 coating in the electron bombardment during the E-sail operation is of concern during missions, which can be as long as 10 years. The emissivity measurement setup was designed so that the tether wire can be irradiated with electron flux in the same vacuum chamber. This enables the measurement of the emissivity before and after electron bombardment without exposing the wire to atmospheric pressure (see figures 7 and 8).

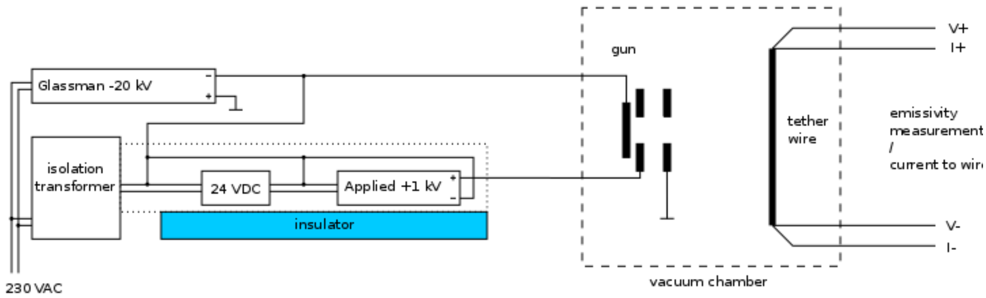

Figure 7. Schematic presentation of the measurement setup. During the electron bombardment the tether wire current is measured from the same feedthroughs, which are used for emissivity measurement.

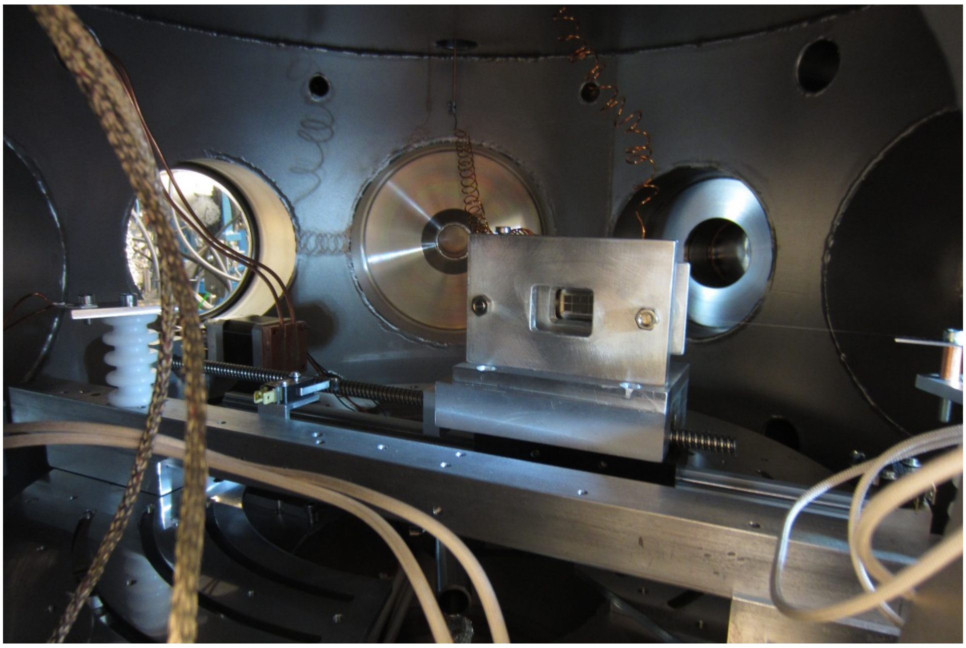

Figure 8. Photograph from inside the vacuum chamber.

Originally (in D23.2) the experiment was sketched to be based on a thermionic filament electron gun. Unfortunately this approach proved problematic due to the evaporation of the filament material on the tether wire during bombardment. Therefore a field-emission electron gun, which has been developed at the University of Jyväskylä for E-sail related nanosatellites, was selected to be used instead. With a thermionic gun a coaxial design could be used to provide a wide electron beam. The field-emission guns are flat. Because of this and due to limited vacuum-chamber size a movable electron gun had to be selected instead of electrostatic beam sweeping to cover the length of the wire. Unfortunately that choice also has an effect on the maximum electron beam intensity which can be run to the tether wire.

A 50 μA, 10 keV, 10x10 mm^2 electron beam from the electron gun hitting the 50 μm diameter tether wire brings a heat flux of 250 nA·10 kV = 2.5 mW to the wire. According to thermodynamic simulations this is enough to bring the local temperature of the wire to about 570 K. Therefore the beam power density should be limited to about this level. The average flux, for the 0.5 m wire sample in this case is 500 nA/m, which is only 100-times higher than the flux in space (0.1 mA for 20 km tether, i.e. 5 nA/m). It is not therefore possible to bombard the tether wire with a total fluence equal to a 10 year mission.

The test was started with 500 nA/m level, but during the experiment, the field emission electron gun performance degraded due to poor vacuum conditions. The test was continued for 48 hours and the average flux used was about 250 nA/m. The total electron fluence received by the wire is equivalent to 100 days in solar wind at 1 AU distance from the sun. The emissivity was measured before the electron bombardment, after 24 hours and after 48 hours, when the experiment was ended. The deviations in the measured emissivities were small and are thought to arise from measurement uncertainties (see figure 9).

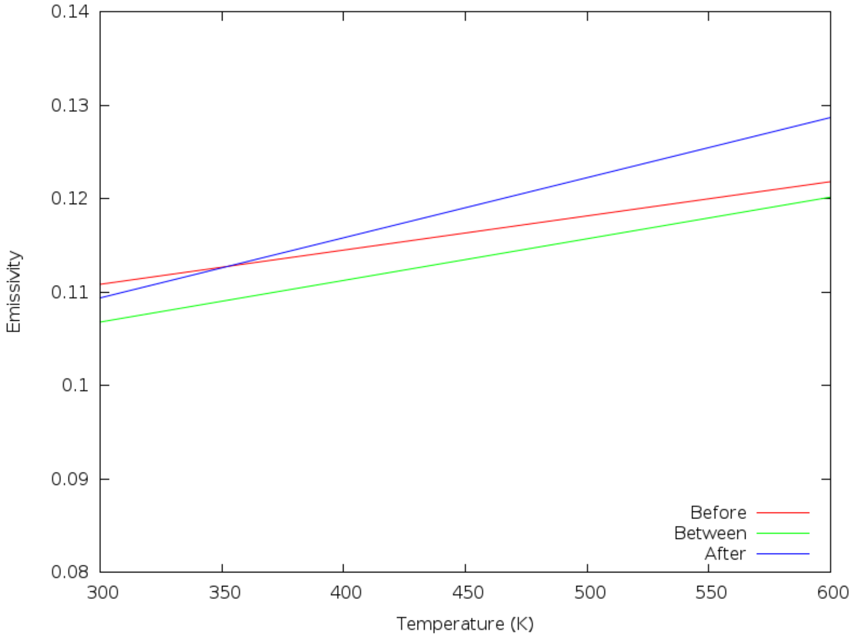

Figure 9. The emissivity of the tether wire before the electron bombardment, after 24 hours (between) and after the full 48 hours of bombardment. The deviations of the emissivity is within the measurement uncertainties.

During this work it was learned that the experimental conditions were not applicable for evaluating the durability of the E-sail tethers in space. First of all, the vacuum level in the experimental chamber was only $3 \cdot 10^{-6}$ mbar during electron bombardment tests because of outgassing from the motor. Therefore the density of oxygen in the surrounding atmosphere is sufficient to provide a repair process, if the tether coating becomes oxygen deficient. Also the tether wire was unbiased in the experiment, which may in turn increase the creation of holes in the oxide layer. In the E-sail the tether is biased positively and low-energy secondary electrons ejected from the wire will return to the surface and possibly fill the electron holes.

4. Collision of two tethers

4.1. Motivation

If a tether breaks while the E-sail is in operation, the tether gets neutralized in roughly 30 s time by the solar wind electrons. If the broken tether then collides with another tether that is still biased, it is possible that further damage occurs because of the discharge between the tethers. Possible scenarios are: a) the working tether will be cut, b) the loose tether will welded to the working tether, c) nothing happens. The situation was first studied by simulation and then with an experimental approach.

4.2. Computer modelling

In this approach we assumed that two wires collide with a 20 kV potential difference. The relevant time scale for the discharge process is so short and the instantaneous currents are so high that the power supply doesn't have time or capability to react to it. The discharge is dominated by the charge flowing from the capacitance of the other wire to the capacitance of the other wire. The system is therefore characterized by the tether wire capacitance, resistance and inductance. In reality the system is highly dynamic as the voltage difference between the colliding wires varies as the charges fills the local capacitance. Also the inductance plays a role as the dI/dt is very high. In the simple model used in this work the capacitance of a tether has been estimated with an infinite length cylindrical capacitor model with outer radius of Debye length of the solar wind plasma (26 m) and inner diameter of one 50 μm wire. The difference of capacitance between one-wire capacitor and N-wire hoy-/hey-tether system has been estimated to be negligible. From this starting point we have calculated that the capacitance of the tether is about 4 pF/m. The resistance of the tether in the calculation has been assumed to be the resistance of a 50 μm thick aluminum wire. The hoy-/hey-tether structure is not taken in account. This results in 14 Ω/m resistance. The inductance is not taken in account.

The time dependence of the discharge was calculated numerically using the capacitance and resistance values and assuming a total length of 20 km for the wire. The contact was assumed to happen in one end (this is not the worst case scenario, because the total instantaneous current would be double at the middle of the wire). The contact discharge current was found to be almost independent of the contact resistance as long as the contact resistance was <100 Ω. The discharge current is shown in figure 10.

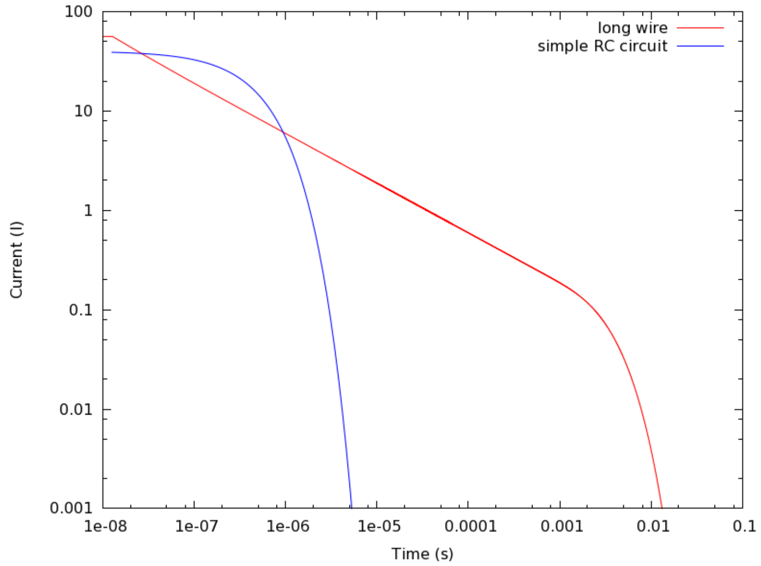

Figure 10. Discharge current from 20 km wire initially biased to 20 kV short circuited to ground (red curve) and discharge of a simple RC circuit with R=500 Ω and C=1 nF.

The discharge power is mainly dissipated on the positively biased tether at the point where discharge electrons hit the wire. It is assumed that the current carried by positive ions is negligible. Therefore it is sufficient to calculate the thermal effects only on the positively biased wire. The discharge current was therefore converted to power assuming a fixed "contact" resistance. The power was dumped into the wire on a volume of certain length, which is about the size of the estimated discharge area. The diffusion of heat out of the point of discharge and radiative heat losses were then simulated with a 1D heat equation solver. The wire (initially at some temperature) reaches a maximum temperature at the discharge point due to the power dissipated at the contact before the heat is diffused further away. The maximum temperature rise of the wire was recorded in the simulation.

The length of wire receiving the discharge can be estimated with some accuracy to be around 5-20 μm. The contact resistance is a more problematic parameter to estimate and unfortunately the maximum temperature reached is quite sensitive to this parameter. The numbers used in the simulations (0.1-0.5 Ω) are based on practical experience with high voltage discharges. In the cases observed the instantaneous currents of kV-range discharges are often in the 1000 A-range small diameter wires touching each other. Pure aluminium wire unfortunately might behave quite differently because of the oxidation layer on it and the effect of vacuum vs. air is difficult to take in account. The contact resistance is assumed to be fixed and the change of resistivity as a function of temperature is not taken in account because it is believed that other factors play a more important role in the system being modelled. The results are shown in table 2. The results show that the tether wire peak temperatures are close to the melting point. Because of this and the quite strong approximations in the model it is difficult to draw any conclusions. The tether wire may or may not break/weld together in an event of collision.

Table 2. Maximum temperature rise on wire. Aluminum melts at 933 K so if we assume a T=300 K before collision, the melting will happen at ΔT=633 K.

ΔT (K)	Contact length (μm)		
Contact resistance (Ω)	5	10	20
0.1	350	245	161
0.2	699	490	322
0.3	1049	613	483
0.5	1749	1226	805

4.3. Experimental approach

The next approach to this problem was an experimental one. A charge storage device made from 500 Ω resistor and 1 nF capacitor was made. A holder was constructed for one aluminium wire in ground potential and another high voltage compatible holder for the other wire. The wires were perpendicular to each other in the holders (see figure 11). The holders were placed inside a vacuum chamber with a motion feedthrough for enabling collision of the wires. The vacuum chamber was pumped to $3 \cdot 10^{-7}$ mbar. The charge storage device was loaded to +17.5 kV potential, which corresponds to 25 % smaller energy compared to +20 kV. Unfortunately the high voltage unit used couldn't go to +20 kV. The wires were run into contact. A visible spark was observed between the wires on collision.

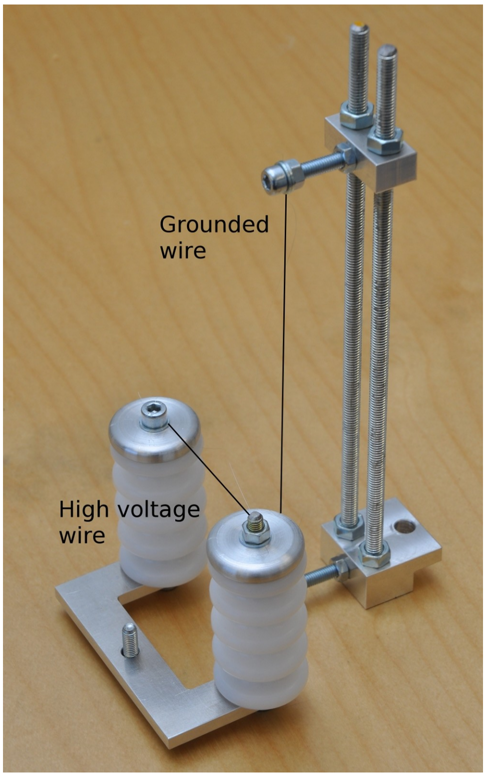

Figure 11. Experimental setup used for the wire collision experiments. During the tests the equipment was placed inside a vacuum chamber.

The 25 μm diameter wires were observed to break on the first collision. 50 μm diameter wire lasted for three collisions after which one of the wires broke (the breaking wire was the wire on the positive high voltage, which gets higher energy impact as fast electrons hit it during the spark). The experiment was repeated with another 50 μm wire using the full internal capacitance of the power supply (7.5 nF). This resulted in welding and breakage of the wires on the first collision. The points of collision were studied with scanning electron microscope (SEM) after the experiments and evidence of wires melting was observed (see figure 12).

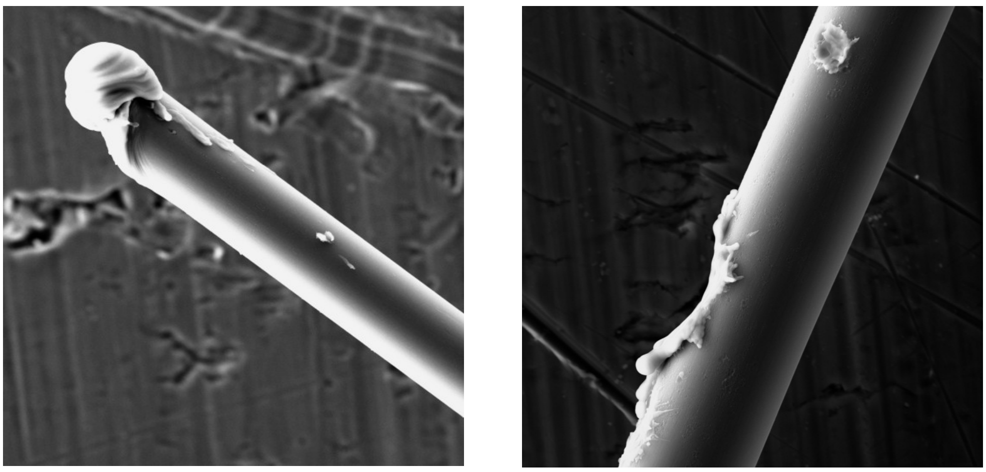

Figure 12. End of broken wire on left (was on positive high voltage) and point of contact on the other wire on the left (grounded wire).

According to these experiments it is possible that the tether survives a collision with another charged tether. On the other hand it is also possible that the tether breaks because of such a collision. Unfortunately the working tethers on the satellite are in positive high voltage with respect to the floating tether and therefore it will experience a higher energy impact than the other tether. When estimating the possibility of a wire breaking in the satellite, it should be remembered that there is tension on the tethers, which makes the situation harder for the wires. In the experiments there was no tension in the wires.

According to the experiments it is possible that a spark with a total energy and time scale in the range, which is probable in the satellite tether collision, can break the tether. Therefore measures should be taken to prevent the collisions of tethers with high potential difference.

5. Conclusions

The main conclusions from this work are

- The emissivity of the tether wire with the current ALD coating process is between 0.05 and 0.1 at temperatures between 300 and 600 K. It is not equal to bulk aluminium oxide emissivity.

- The tether may break due to high voltage sparks. Measures should be taken to prevent collisions of tethers with high potential difference.

- The oxide layer on the tether wire might turn to bare aluminium due to electron bombardment induced oxygen loss. This effect is difficult to study in a laboratory.

References

[1] Engineering toolbox (http://www.engineeringtoolbox.com/radiation-heat-emissivity-aluminum-d_433.html), November 2013.

[2] Mikron. Table of emissivity of various surfaces for infrared thermometry, (http://www-eng.lbl.gov/~dw/projects/DW4229_LHC_detector_analysis/calculations/emissivity2.pdf), November 2013.

[3] National Institute of Standards and Technology, ESTAR Program, (http://physics.nist.gov/PhysRefData/Star/Text/ESTAR.html), November 2013.

[4] R. C. Weast, Handbook of Chemistry and Physics, CRC Press, 1975.